Article

Cell Reports

# An Activating STAT3 Mutation Causes Neonatal Diabetes through Premature Induction of Pancreatic Differentiation

## Graphical Abstract

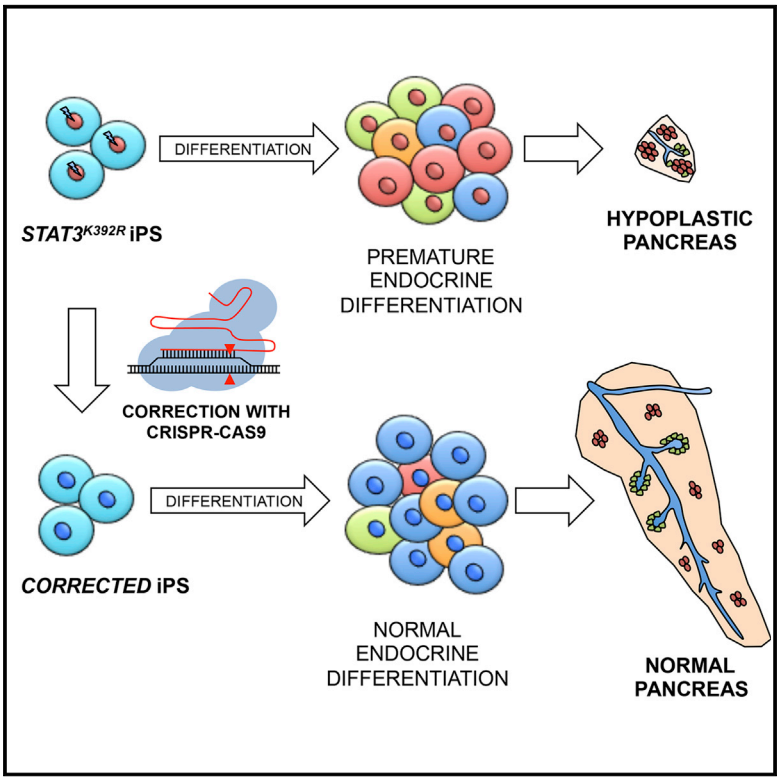


## Highlights

- iPSCs derived from a neonatal diabetes patient with an activating STAT3 mutation
- Mutant cells show premature endocrine differentiation through *NEUROG3* upregulation
- Disease phenotype normalized by CRISPR/Cas9 mutation correction
- Mechanism involves increased nuclear shuttling of mutant STAT3

## Authors

Jonna Saarimäki-Vire, Diego Balboa, Mark A. Russell, ..., Markku Varjosalo, Noel G. Morgan, Timo Otonkoski

## Correspondence

jonna.saarimaki@helsinki.fi (J.S.-V.), timo.otonkoski@helsinki.fi (T.O.)

## In Brief

Saarimäki-Vire et al. use iPSCs derived from a patient with permanent neonatal diabetes to demonstrate that an activating STAT3 mutation leads to premature *NEUROG3* expression and concomitant differentiation of pancreatic progenitors through increased nuclear shuttling of the mutant protein.

Saarimäki-Vire et al., 2017, Cell Reports *19*, 281–294
April 11, 2017 
http://dx.doi.org/10.1016/j.celrep.2017.03.055

Cell Reports
Article



# An Activating STAT3 Mutation Causes Neonatal Diabetes through Premature Induction of Pancreatic Differentiation

Jonna Saarimäki-Vire,[1,8,9,*] Diego Balboa,[1,8] Mark A. Russell,[2] Juha Saarikettu,[3] Matias Kinnunen,[4] Salla Keskitalo,[4] Amrinder Malhi,[2] Cristina Valensisi,[5] Colin Andrus,[5] Solja Eurola,[1] Heli Grym,[1] Jarkko Ustinov,[1] Kirmo Wartiovaara,[1,7] R. David Hawkins,[5] Olli Silvennoinen,[3] Markku Varjosalo,[4] Noel G. Morgan,[2] and Timo Otonkoski[1,6,*]

[1]Research Programs Unit, Molecular Neurology and Biomedicum Stem Cell Centre, Faculty of Medicine, University of Helsinki, 00014 Helsinki, Finland
[2]Institute of Biomedical and Clinical Science, University of Exeter Medical School, Exeter EX2 5DW, UK
[3]Faculty of Medicine and Life Sciences, University of Tampere, and Tampere University Hospital, 33014 Tampere, Finland
[4]Molecular Systems Biology Research Group, Institute of Biotechnology, University of Helsinki, 00014 Helsinki, Finland
[5]Division of Medical Genetics, Department of Medicine, Department of Genome Sciences, Institute for Stem Cell and Regenerative Medicine, University of Washington School of Medicine, Seattle, WA 98109, USA
[6]Children's Hospital, University of Helsinki and Helsinki University Hospital, 00290 Helsinki, Finland
[7]Clinical Genetics, HUSLAB, Helsinki University Central Hospital, Haartmaninkatu 4, 00290 Helsinki, Finland
[8]These authors contributed equally
[9]Lead Contact
*Correspondence: jonna.saarimaki@helsinki.fi (J.S.-V.), timo.otonkoski@helsinki.fi (T.O.)
http://dx.doi.org/10.1016/j.celrep.2017.03.055

## SUMMARY

**Activating germline mutations in *STAT3* were recently identified as a cause of neonatal diabetes mellitus associated with beta-cell autoimmunity. We have investigated the effect of an activating mutation, STAT3$^{K392R}$, on pancreatic development using induced pluripotent stem cells (iPSCs) derived from a patient with neonatal diabetes and pancreatic hypoplasia. Early pancreatic endoderm differentiated similarly from *STAT3*$^{K392R}$ and healthy-control cells, but in later stages, *NEUROG3* expression was upregulated prematurely in *STAT3*$^{K392R}$ cells together with insulin (INS) and glucagon (GCG). RNA sequencing (RNA-seq) showed robust *NEUROG3* downstream targets upregulation. *STAT3* mutation correction with CRISPR/Cas9 reversed completely the disease phenotype. STAT3$^{K392R}$-activating properties were not explained fully by altered DNA-binding affinity or increased phosphorylation. Instead, reporter assays demonstrated *NEUROG3* promoter activation by STAT3 in pancreatic cells. Furthermore, proteomic and immunocytochemical analyses revealed increased nuclear translocation of STAT3$^{K392R}$. Collectively, our results demonstrate that the STAT3$^{K392R}$ mutation causes premature endocrine differentiation through direct induction of *NEUROG3* expression.**

## INTRODUCTION

The pancreas is a multifunctional organ, consisting of two functionally distinct compartments that originate from the posterior foregut endoderm. The acinar and ductal cells of the exocrine compartment are derived from the tip and trunk regions of the branched pancreatic epithelium, respectively (Jennings et al., 2015; Pan and Wright, 2011; Puri et al., 2015). The endocrine pancreas develops from trunk cells that upregulate Neurogenin3 (NEUROG3). These cells delaminate from the pancreatic epithelium to form the islets of Langerhans. The islets contain five major endocrine cell types that regulate nutrient metabolism and glucose homeostasis and secrete glucagon (α), insulin (β), somatostatin (δ), ghrelin (ε), or pancreatic polypeptide (γ). Elucidation of the molecular mechanisms controlling the development and function of these cells is essential to an improved understanding of the underlying causes of diabetes, a major global health problem (WHO, 2016).

Signal transducer and activator of transcription 3 (STAT3) is a critical component of cytokine signaling that regulates a diversity of cellular processes. The role of STAT3 has been best established in the immune system (O'Shea and Plenge, 2012), where it mediates the transcriptional responses to several cytokines (e.g., interleukin-6 [IL-6], IL-10, and leukemia inhibitory factor [LIF]) acting via receptors coupled to members of the Janus kinase (JAK) family, which in turn phosphorylate STAT proteins. The STAT protein family is composed of seven distinct members that can form homo- and heterodimers. Dimerization leads to their nuclear translocation and thence to modulation of the transcription of target genes (O'Shea et al., 2013). Genetic deletion of *Stat3* in mice leads to early embryonic lethality (Takeda et al., 1997).

STAT3 also has important functions outside the immune system. For example, pancreas-specific (*Pdx1-Cre*) inactivation of the *Stat3* gene in mice causes defects in the development and function of the pancreas, presenting mainly as a diminished microvascular network in the islets (Kostromina et al., 2010, 2013; Lee and Hennighausen, 2005). However, beta-cell-specific

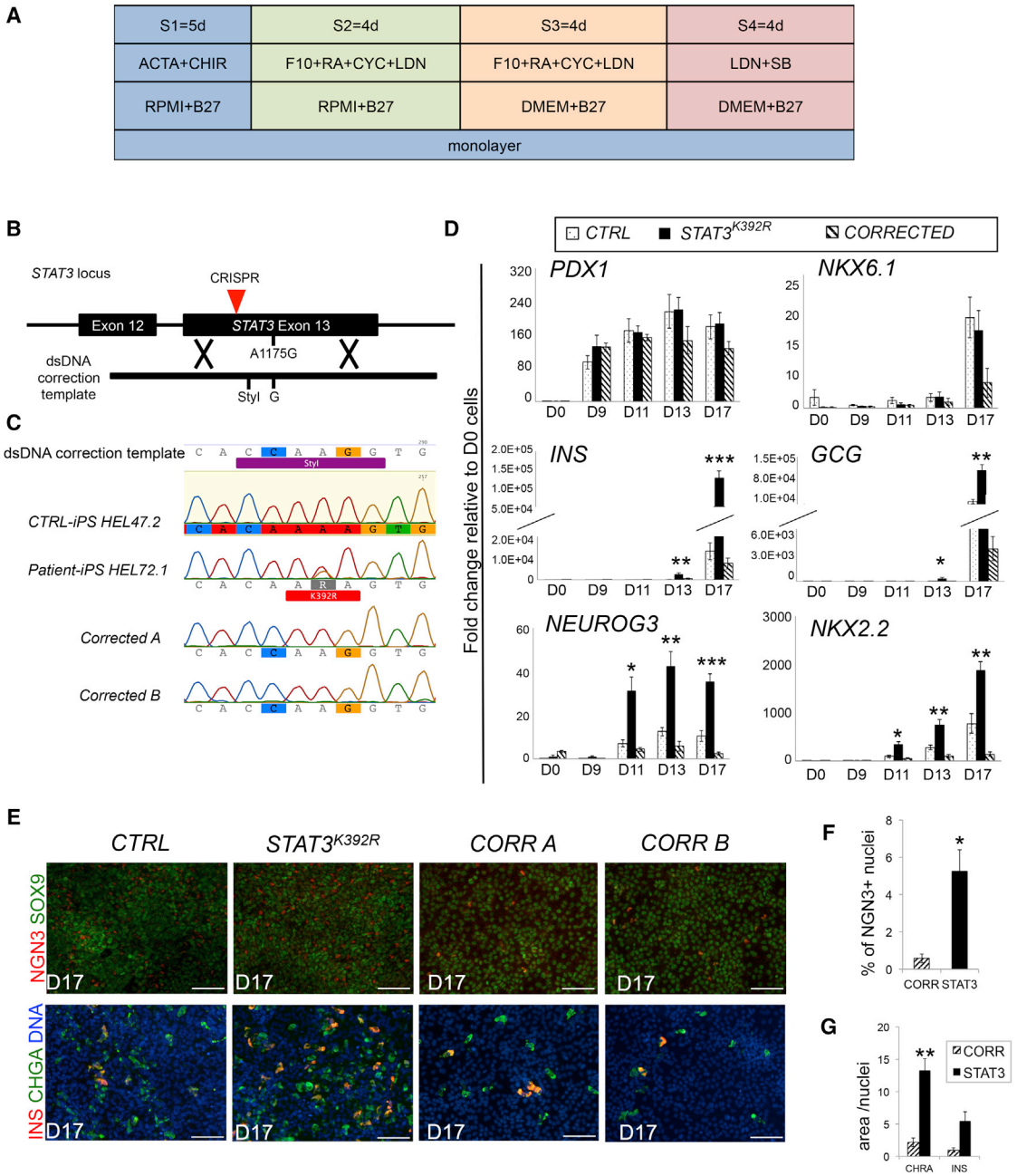


**Figure 1. Correction of STAT3$^{K392R}$ Mutation with CRISPR/Cas9 Rescues the Premature Differentiation Phenotype**

(A) Seventeen-days differentiation protocol (see Experimental Procedures for details). Abbreviations: ACTA, activin A; B27, B-27 supplement; CHIR, CHIR-99021, GSK-3 inhibitor; CYC, cyclopamine; F10, fibroblast growth factor 10; LDN, LDN-193189 Alk inhibitor; RA, retinoid acid; RPMI, RPMI-1640 medium. No SB was used during stages 2 and 3 in this protocol.

(B) Schematic presentation of the targeting strategy for CRISPR/Cas9-mediated mutation correction. See also Figure S3.

(C) DNA sequences of correction template, *STAT3*$^{K392R}$, and *CORRECTED* cell lines. See also Figure S6.

(D) Relative gene expression of pancreatic genes in *CTRL* (n = 8–15/stage independent experiments; two different cell lines), *STAT3*$^{K392R}$ (n = 7–12/stage independent experiments; three different cell lines), and *CORRECTED* (n = 3; three different *CORRECTED* clones) cells. Data represent the mean ± SEM. Statistical analysis was performed with one-way ANOVA followed by Tukey's test. Significant differences between *STAT3*$^{K392R}$ (*STAT3*) cells relative to control (*CTRL*) and *CORRECTED* cells are shown as *$p < 0.05$, **$p < 0.01$, and ***$p < 0.001$. See also Figure S4.

(E) Double immunocytochemistry for NEUROG3 (NGN3) plus SOX9 and INSULIN plus CHROMOGRANIN A in *CTRL*, *STAT3*$^{K392R}$, and two corrected lines after 17 days differentiation. The scale bar represents 100 μm. See also Figure S5.

*(legend continued on next page)*

*Stat3* mouse knockout yields more severe functional defects, including altered secretion of insulin and improper islet organization (Gorogawa et al., 2004). In the adult pancreas, STAT3 signaling is critical for the regeneration of beta cells (Baeyens et al., 2014; Valdez et al., 2016).

The common polygenic forms of diabetes do not present during the first 6 months of life, but rare cases of permanent neonatal diabetes (PNDM) can occur during this period. These are caused by mutations in genes important for pancreatic beta cell development or function. Mutations in 22 distinct genes have been associated with monogenic forms of diabetes (De Franco and Ellard, 2015; Murphy et al., 2008), and recently, activating *STAT3* mutations were identified as a cause of PNDM in association with early onset autoimmunity. The most highly activating mutation, K392R (identified in a Finnish patient), was found to correlate with the most severe clinical phenotype and was localized in the DNA binding domain of STAT3 (Flanagan et al., 2014). The patient presented with high levels of beta-cell autoantibodies at birth (Otonkoski et al., 2000), associated with exocrine insufficiency and pancreatic hypoplasia, along with a general growth defect. Later, the patient developed an autoimmune lung disease, celiac disease-like enteropathy, and large granular lymphocyte (LGL) leukemia (Haapaniemi et al., 2015). Based on the strong immunological phenotype, diabetes was presumed to be the result of an autoimmune attack on the endocrine pancreas. However, we hypothesized that the STAT3$^{K392R}$ mutation could also directly interfere with pancreatic development and thereby cause the pancreatic hypoplasia. In this study, we have used patient-derived induced pluripotent stem cells (iPSCs) to test this hypothesis. Our results show that, when induced to differentiate into pancreatic progenitors, the *STAT3*$^{K392R}$ cells undergo premature endocrine differentiation due to activation of the pro-endocrine transcription factor NEUROG3. The mechanism of this effect is based on the increased nuclear shuttling of the mutated protein.

## RESULTS

### Patient-Derived iPSCs with an Activating STAT3 Mutation Differentiate Prematurely to the Pancreatic Endocrine Lineage

We derived iPSC lines from the dermal fibroblasts of a patient with the STAT3 K392R mutation by retroviral delivery of reprogramming factors OCT4, SOX2, CMYC, and KLF4, as described elsewhere (Toivonen et al., 2013a). Characterization of three different iPSC lines after propagation for at least ten passages demonstrated the expression of hallmark pluripotency markers, the silencing of the retroviral promoters, and pluripotent differentiation in vitro by embryoid body assay (Figure S1). DNA sequencing of the STAT3 exon 2 verified the presence of the heterozygous A to G nucleotide change causing the K392R missense mutation in the patient-derived iPSCs (Figure 1C).

The patient-derived iPSC lines (*STAT3*$^{K392R}$ cells) were then differentiated into pancreatic progenitors using a four-stage protocol based on previously published reports (Mfopou et al., 2010; Nostro et al., 2011; Toivonen et al., 2013b) with minor modifications to achieve efficient differentiation from all the cell lines (Figure S2A; Supplemental Experimental Procedures). Healthy-donor iPSC line HEL47.2 (Trokovic et al., 2015a), HEL24.3 (Trokovic et al., 2015b), HEL46.11 (Achuta et al., 2017), and human embryonic stem cell line H9 (Thomson et al., 1998) were used as controls.

Both *STAT3*$^{K392R}$ and control cell lines differentiated successfully to definitive endoderm (DE) as shown by cell morphology and the expression of CXCR4 (Figures S2B, S2C, and S4C), FOXA2, and SOX17 (Figures S4A and S4B). All cell lines also progressed efficiently through primitive gut tube (day 9), posterior foregut (day 11), and pancreatic endoderm (day 13) stages to the final pancreatic progenitor (day 17) stage, where they expressed PDX1 homogeneously (Figure S2D). qRT-PCR analysis across the different stages confirmed that *PDX1* and *NKX6.1* followed similar expression levels and kinetics in mutant and control cells (Figure S2E). Interestingly, we found that pancreatic endocrine cell markers *NEUROG3* and insulin (*INS*) were significantly upregulated in the *STAT3*$^{K392R}$ cells (Figures S2F, S2J, and S2K). Immunocytochemical quantification also revealed increased numbers of INS+ cells (Figures S2G–S2I) at day 17.

### Correction of the STAT3 Mutation Rescues the Premature Differentiation Phenotype

The genetic background of the somatic cell donor has been shown to affect the capability of reprogrammed iPSCs to differentiate efficiently into particular cell types (Choi et al., 2015; Kyttälä et al., 2016). It is possible, therefore, that differences in the differentiation efficiency of the iPSCs derived from the patient versus healthy controls might disguise a mutation-specific phenotype when using comparative differentiation protocols in vitro. To overcome this problem and verify the premature differentiation phenotype, we corrected the STAT3$^{K392R}$ mutation in the patient iPSCs using CRISPR/Cas9 genome-editing technology. Several guide RNAs (gRNAs) were designed to target the *STAT3* locus near the mutation site and their efficiency tested in HEK293 cells (Figure S3). After several efficiency tests (Figure S3; Supplemental Experimental Procedures), we decided to use wild-type (WT) Cas9 (gRNA STAT3.3) combined with a PCR-generated double-stranded DNA (dsDNA) correction template to repair the mutation by homologous recombination. The 202-base-pair dsDNA template corrected the A to G mutant change and introduced a silent nucleotide change, creating a new restriction site (StyI) for screening purposes (Figures 1B and S3B). After single-cell cloning of the electroporated patient iPSCs by EGFP+ single-cell sorting (cloning efficiency of 45.4% ± 14.5% SD; n = 6; see Supplemental Experimental Procedures), we were able to isolate several distinct iPSC lines

(F) Quantification of NEUROG3+ cells in *STAT3*$^{K392R}$ (n = 3; three different clones) and *CORRECTED* cells (n = 3; three different corrected clones) at day 17 of differentiation. Data represent the mean ± SEM. Statistical analysis was performed with Student's t test. *$p < 0.05$.
(G) Quantification of CHGA+ and INS+ cells in *STAT3*$^{K392R}$ (n = 3; three different clones) and *CORRECTED* cells (n = 3; three different corrected clones) at D17 of differentiation. Data represent the mean ± SEM. Statistical analysis was performed with Student's t test. **$p < 0.01$.

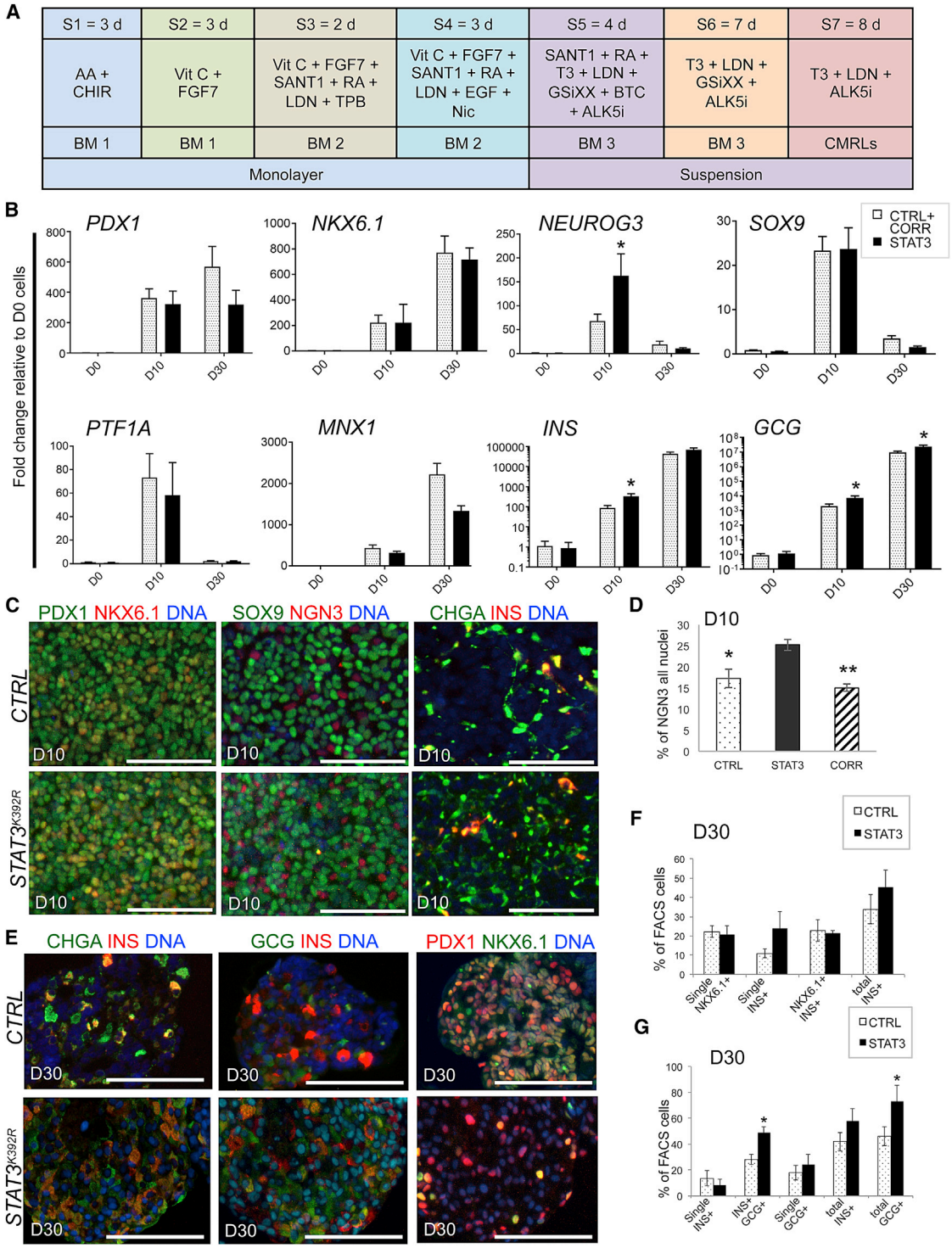


**Figure 2. Extended Differentiation into Islet-like Aggregates**

(A) Protocol for extended differentiation (for abbreviations, see Supplemental Experimental Procedures).

(B) Gene expression levels analyzed by qRT-PCR of pancreatic genes in *CTRL* (n = 4; pooled data from two healthy-donor control lines and two *CORRECTED* clones) and *STAT3*$^{K392R}$ (four independent experiments) cells. Data represent the mean ± SEM. *p < 0.05; Student's t test. Note the logarithmic scale for *INS* and *GCG*.

(C) Immunocytochemistry analysis for PDX1, NKX6.1, SOX9, NEUROG3, CHGA, and INS after D10 differentiation in monolayer, in *CTRL* (healthy donor) *STAT3*$^{K392R}$ cells. The scale bars represent 100 μm.

*(legend continued on next page)*

(5.3%; 12 out 225 clones) that presented either heterozygous or homozygous recombination with the donor template, correction of the STAT3$^{K392R}$ mutation, and no Cas9-induced mutations in the other allele (Figures 1C and S3A). The corrected cell lines A, B, and C were karyotypically normal and did not present mutations in putative off-target sites and therefore were used for subsequent experiments (Figures S6A and S6B; Table S1).

The early upregulation of *INS* in the *STAT3$^{K392R}$* cell lines suggests that the kinetics of endocrine lineage differentiation might be altered in these cells. Some pancreatic differentiation protocols have been optimized to obtain higher numbers of INS+ cells by inducing the expression of *NEUROG3* via inhibition of transforming growth factor β (TGF-β) signaling. Because this could interfere with the effect of STAT3$^{K392R}$, we omitted the TGF-β inhibitor SB from stages 2 and 3 of our protocol (Figure 1A) and differentiated the STAT3-corrected iPSCs together with the *STAT3$^{K392R}$* and control iPSCs. The corrected cell lines also differentiated efficiently to definitive endoderm (analyzed by cytometry for CXCR4+ cells in Figure S4C), pancreatic endoderm, and progenitors as shown by immunocytochemistry (Figures S4D, S4E, and S5).

As expected, omission of TGF-β inhibition resulted in decreased levels of *NEUROG3*, *INS*, and *GCG* at early time points (d11 and d13) in control cells (compare Figure 1D with S2F). Interestingly, the levels of endocrine markers *NEUROG3*, *NKX2.2*, *INS*, and *GCG* were again distinctly higher in the *STAT3$^{K392R}$* cells than in the control and corrected cells (Figure 1D). Remarkably, the corrected iPSCs showed similar expression levels to controls, indicating that correction of the K392R mutation had rescued the premature endocrine differentiation phenotype (Figure 1C). The results were identical with three independent corrected clones (immunocytochemistry of differentiated individual clones presented in Figures S4 and S5). These findings were further confirmed by quantification of the cells expressing NEUROG3, CHGA, and INS (Figures 1E–1G).

We then differentiated the cells further in order to obtain more mature beta cells, using a protocol modified from the ones described by Pagliuca et al. (2014) and Rezania et al. (2014; Figure 2A; Supplemental Experimental Procedures). Similar to that observed with the shorter differentiation protocols, significant differences were observed in the expression of *NEUROG3* in the pancreatic progenitor stage (d10) in the *STAT3$^{K392R}$* cells compared with control and corrected cells (*CTRL* + *CORR*; Figure 2B). More abundant NEUROG3+ cells were also detected by immunocytochemistry at d10 (Figures 2C and 2D). At the islet-like stage (d30), the expression of *GCG* was significantly upregulated in the *STAT3$^{K392R}$* cells (Figure 2B), which presented abundant endocrine cells (Figure 2E). Quantification by flow cytometry at d30 revealed that there were no differences in the numbers of INS+ or NKX6.1+ cells (Figure 2F), whereas the numbers of INS/GCG (glucagon) double-positive and total GCG+ cells were significantly increased in the *STAT3$^{K392R}$* (Figure 2G). Thus, this optimized protocol also showed that *STAT3$^{K392R}$* cells upregulated *NEUROG3* prematurely, resulting in increased endocrine differentiation, which was biased toward the GCG+ alpha cell lineage.

To examine the possible genes and pathways causing the premature endocrine differentiation in *STAT3$^{K392R}$* iPSCs, we performed RNA-seq at day 11 of differentiation with the modified protocol. In mutant versus corrected cells, 777 genes were upregulated and 206 downregulated (fold change ≥ 1.5; Table S2). Ingenuity pathway analysis showed that among the most significantly upregulated genes in the mutant versus corrected cells were *NEUROG3* and its downstream targets (Figure 3A). It also suggested that NEUROG3 is the main putative upstream regulator of the detected overexpressed genes (Figure 3B). No significant changes were detected in genes or pathways known to regulate NEUROG3 (e.g., Notch or TGF-β signaling pathways) or other endocrine markers (Table S2). We performed gene ontology (GO) analysis on the differentially expressed genes to identify biological processes associated with *STAT3$^{K392R}$*. Consistent with the increased endocrine cell differentiation, genes differentially expressed in *STAT3$^{K392R}$* were associated with ion transport, transmembrane transport, synaptic signaling, and RNA biosynthesis (Figure S6C). These results demonstrate that the activating *STAT3$^{K392R}$* mutation drives pancreatic progenitors to differentiate into endocrine cells by inducing the premature expression of NEUROG3.

## The Mutant Phenotype Is Not Explained by Differential Phosphorylation of STAT3

Activation of STAT3-mediated signaling pathways with IL-6 has previously been shown to increase *NEUROG3* expression and differentiation toward endocrine lineage (Gutteridge et al., 2013). To determine whether ligands for STAT3 signaling would induce NEUROG3 expression, we studied the phosphorylation status of ectopically expressed *WT* and mutant STAT3 in HEK293 cells. Cells were either left untreated or stimulated with IL-6 or LIF, known inducers of the STAT3 signaling pathway (Baeyens et al., 2006, 2014). Under non-stimulating conditions, the phosphorylation of residue Y705 was increased in STAT3$^{K392R}$-transfected cells (Figure S7A). As shown previously, the STAT3$^{K392R}$ was more transcriptionally active than STAT3 WT in HEK293 under both basal and IL-6-stimulated conditions using a STAT3-luciferase reporter assay (Figure S7B; Flanagan et al., 2014). Interestingly, mutagenesis of the Y705 phosphorylation site revealed that the increased transcriptional activity of STAT3$^{K392R}$ depends only partially on Y705 phosphorylation. A

(D) Quantification of NEUROG3+ cells in *CTRL* (healthy-donor; n = 3; three different cell lines), *STAT3$^{K392R}$* (n = 4; HEL72D), and *CORRECTED* cells (n = 4; two different corrected clones) at day 17 of differentiation. Statistical analysis was performed with one-way ANOVA followed by Tukey's test. Significant differences between *STAT3$^{K392R}$* (*STAT3*) cells and *CTRL* or *CORRECTED* cells are shown as *$p < 0.05$ and **$p < 0.01$.

(E) Immunohistochemistry analysis for PDX1, NKX6.1, CHGA, INS, and GCG on sections of islet-like clusters at day 30. The scale bars represent 100 μm.

(F) Flow cytometry analysis of dissociated islet-like clusters with NKX6.1 and INS antibodies. Data represent the mean ± SEM.

(G) Flow cytometry analysis of dissociated islet-like clusters with GCG and INS antibodies. Results are presented separately for single- and double-hormone-positive cells. Data represent the mean ± SEM. Student's t test; *$p < 0.05$.

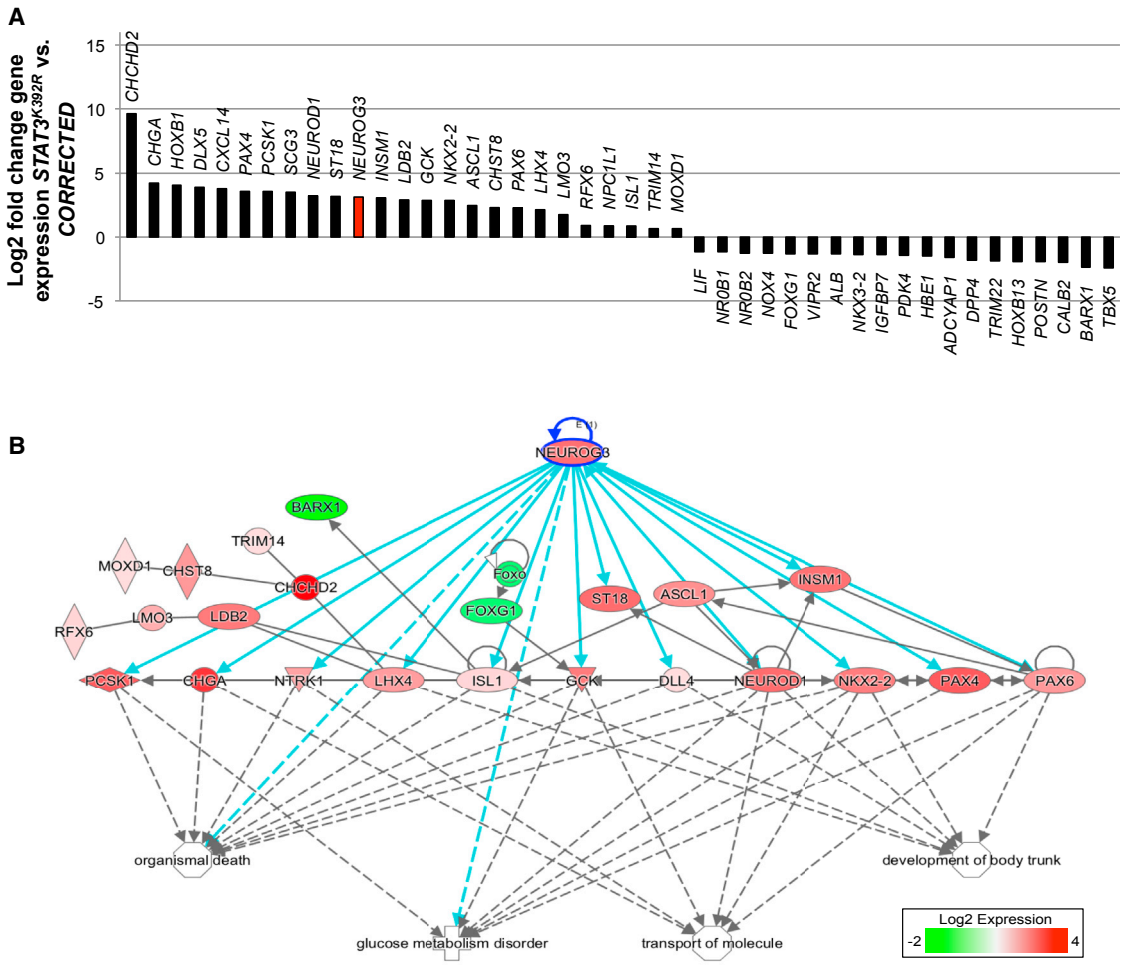


**Figure 3. Differentially Expressed Genes between STAT3$^{K392R}$ and Mutation-Corrected Clones Reveal a NEUROG3-Regulated Network**

(A) The most up- and downregulated genes related with endocrine differentiation in *STAT3*$^{K392R}$ cells. *NEUROG3* levels are marked in red. See also Figure S6.

(B) Interaction network of genes regulated by NEUROG3 differentially expressed in STAT3$^{K392R}$ cells.

Y705-independent activity component was retained in both basal and cytokine-stimulated conditions (Figure S7B).

In order to discover whether activation of STAT3 signaling pathways could mimic the mutation-associated phenotype, we stimulated the differentiating cells with IL-6 or LIF (Baeyens et al., 2014) during stages 2 and 3 (days 5–13; Figure 4A), after confirming that interleukin-6 receptor (IL-6R) was expressed in the cells (Figure S7D). We found that there was no increase of *NEUROG3* expression levels or other endocrine markers upon stimulation (Figure 4A). Because STAT3 signaling status might be cell type and context specific, we also analyzed the phosphorylation of STAT3 at day 11 of differentiation. Although STAT3 Y705 was strongly phosphorylated after IL-6 stimulation (Figures 4B and 4C), in all cell lines, we did not detect significant differences in STAT3 phosphorylation levels between cell lines, with or without IL-6 stimulation. Similar results were observed at the pluripotent stage (Figure S7C).

These results suggest that STAT3 protein phosphorylation is not the main mechanism responsible for the *STAT3*$^{K392R}$ mutation-induced premature endocrine differentiation.

## K392R Mutation Does Not Alter the Intrinsic DNA-Binding Ability of STAT3 to *NEUROG3* Promoter

Electrophoretic mobility shift assay and oligonucleotide pull-down assay were used to analyze the effect of K392R mutation on STAT3 DNA-binding ability. As expected, STAT3 DNA binding was highly dependent on induction of STAT3 phosphorylation by pervanadate stimulation of COS-7 cells as assayed by electrophoretic mobility shift assay (EMSA), where overexpression of STAT3 resulted in an increase in the STAT3 protein-DNA complex (Figure 5A). We did not, however, observe any difference between the DNA-binding efficiency of overexpressed WT and STAT3$^{K392R}$. Similar results were obtained with oligonucleotide pull-downs, where pervanadate treatment caused increased STAT3 DNA binding to the IRF-1 oligo (containing a canonical STAT3-binding motif) to the same degree with WT and STAT3$^{K392R}$ protein (Figure 5B). In HEK293T cells, overexpression of STAT3 was sufficient to induce DNA binding without pervanadate induction (Figure 5C). Importantly, binding to the previously reported STAT3 binding site in the *NEUROG3* promoter sequence (Kaucher et al., 2012) was similar to that at the IRF-1

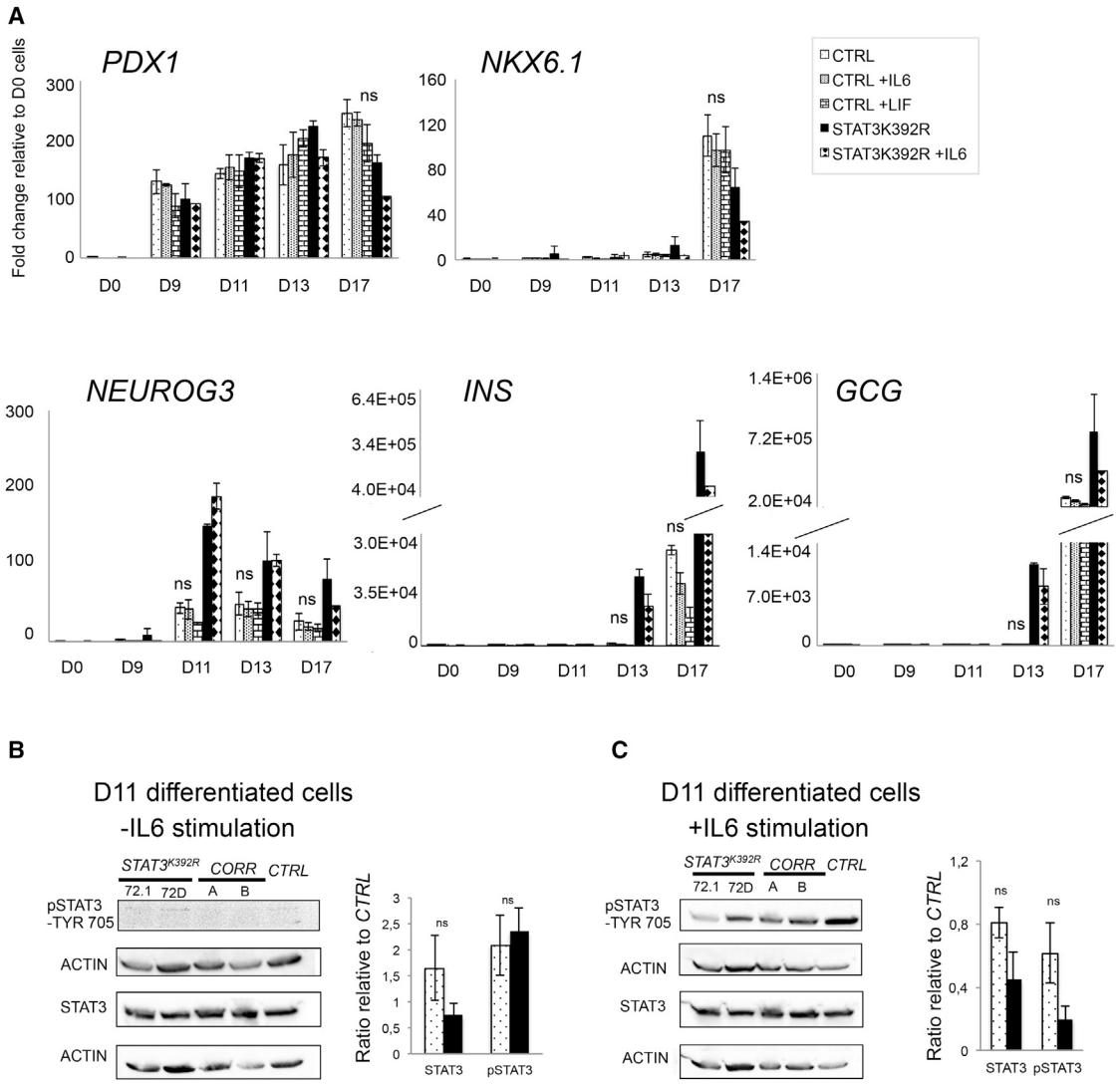


**Figure 4. Premature Differentiation Is Not Caused by Increased STAT3-Y705 Phosphorylation**

(A) Relative gene expression analyzed by qRT-PCR of pancreatic progenitor genes (*PDX1* and *NKX6.1*) and differentiation markers *NEUROG3* (*NGN3*), *INS*, and *GCG* in *CTRL* and *STAT3*$^{K392R}$ cells with and without IL-6 or LIF stimulation during stages 2 and 3 of differentiation to test whether activation of STAT3 signaling pathway is enough to mimic effect of STAT3 mutation. Data represent the mean ± SEM of two to five independent experiments. Statistical analysis with one-way ANOVA did not reveal significant differences between treatment groups.

(B) Western blot analysis of total STAT3 and pSTAT3-Y705 in pancreatic progenitors representing either *STAT3*$^{K392R}$ (two different clones; HEL72.1 and HEL72D) or controls (two corrected lines and one control line) at 11 days of differentiation. Exposure time for STAT3 blots was for 1 s and for pSTAT3 blots 10 min. Quantitative analysis was performed by normalizing values against ACTIN expression, and the data are expressed relative to CTRL. Data represent the mean ± SEM. See also Figure S7.

(C) The same cells as in (B) after IL-6 stimulation for 30 min. Exposure time for STAT3 was 1 s and 22 s for pSTAT3. Quantitative analysis was performed by normalizing values against ACTIN expression, and the data are expressed relative to CTRL. Data represent the mean ± SEM.

sequence, and no difference was observed in the DNA-binding properties of the WT and STAT3$^{K392R}$ proteins (Figures 5B and 5C).

To study further the interaction of STAT3 with the human *NEUROG3* promoter in pancreatic cells, we generated a luciferase reporter construct, which was expressed together with different STAT3 mutants in the PANC1 pancreatic ductal cell line. All three tested STAT3 variants, WT, STAT3$^{K392R}$, and STAT3$^{Y640F}$, a cancer-associated powerfully activating mutant with increased nuclear translocation (Pilati et al., 2011), presented increased *NEUROG3*-luciferase activity without IL-6 stimulation (Figure 5D). STAT3 activity luciferase reporter assay was performed in parallel for comparison (Figure 5E). Activation of the *NEUROG3* promoter was only detectable in PANC1 cells, but not in HEK293 (data not shown). These results show that both WT and mutant STAT3$^{K392R}$ bind to the *NEUROG3*

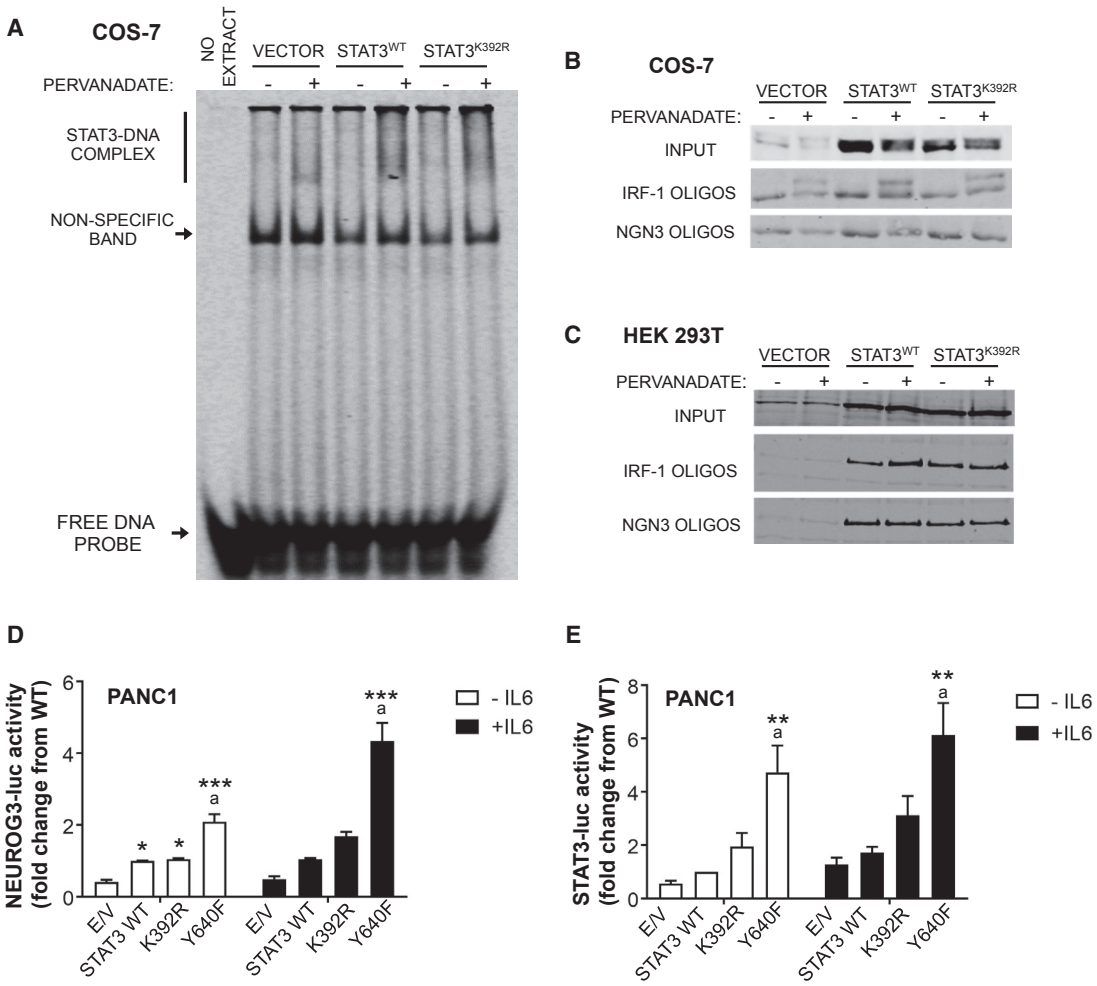


**Figure 5. K392R Mutation Does Not Alter the Intrinsic DNA-Binding Ability of STAT3**

(A) COS7 cells were transfected with an empty vector or expression vector for STAT3 (S3 WT) or STAT3$^{K392R}$ mutant (S3 KR). Cells were stimulated, where indicated, with pervanadate for 20 min to induce STAT3 phosphorylation and nuclear extract used in the binding reaction with an infrared-dye-labeled STAT3 consensus sequence. The complexes were resolved on a native polyacrylamide gel and visualized with LI-COR Odyssey instrument.

(B) Oligonucleotide pull-down with the indicated oligonucleotides using whole-cell extracts of COS-7 cells transfected as in (A). Oligonucleotide-bound proteins were resolved by SDS-PAGE, blotted and detected with a STAT3 antibody.

(C) Oligonucleotide pull-down using whole-cell extracts of HEK293T cells transfected as in (A) and detected by STAT3 immunoblotting.

(D) *NEUROG3* promoter activity in PANC1 cells after transfection of cells with empty vector (E/V), normal STAT3 (STAT3 WT), STAT$^{K392R}$, or STAT3$^{Y640F}$ (highly activating STAT3 mutation) in unstimulated (−IL-6) and stimulated (+IL-6) conditions. Data represent the mean ± SEM of three independent experiments. Statistical significance against empty vector *$p < 0.05$; ***$p < 0.001$; statistical significance against K392R a = $p < 0.05$; one-way ANOVA followed by Tukey's test.

(E) STAT3-regulated SIE (sis-inducible element) promoter activity in PANC1 cells in unstimulated (−IL-6) and stimulated (+IL-6) conditions. Statistics as in (D).

promoter in pancreatic cells and that the STAT3$^{K392R}$-associated increase in *NEUROG3* transcription is not due to an increased DNA-binding affinity.

## K392R Mutation Increases STAT3 Nuclear Localization

Because the disease phenotype could not be fully explained by altered phosphorylation or DNA binding of STAT3$^{K392R}$, we reasoned that the mutation might change the interactions of STAT3 with other proteins. Stable, inducible HEK293 cell lines of WT and STAT3$^{K392R}$ were generated to identify differences in interaction partners by biotin proximity assay (Roux et al., 2012; Figure 6A). Mass spectrometric quantification of the STAT3 interacting partners showed significantly increased interactions with proteins involved in transcriptional regulation (STAT1 [known STAT3 partner], GSE1, TLE3, MTA1, BCOR, and DIDO1) and chromatin remodeling (SMARCC2, YEATS2, SMARCA4, WDR5, and MYSM1) for STAT3$^{K392R}$. Similarly, interaction of STAT3$^{K392R}$ with nuclear pore proteins was elevated (NUP50, NUP62, and NUP153). Additionally, the mutant interacted more effectively with importin subunit alpha-1 (IMA1), whereas its interaction with the export protein RANBP3 was decreased (Figure 6A). Analysis of the phospho-modified peptides showed similar degree of phosphorylation on S727 (15.6% for STAT3$^{K392R}$ versus 10.7% for WT).

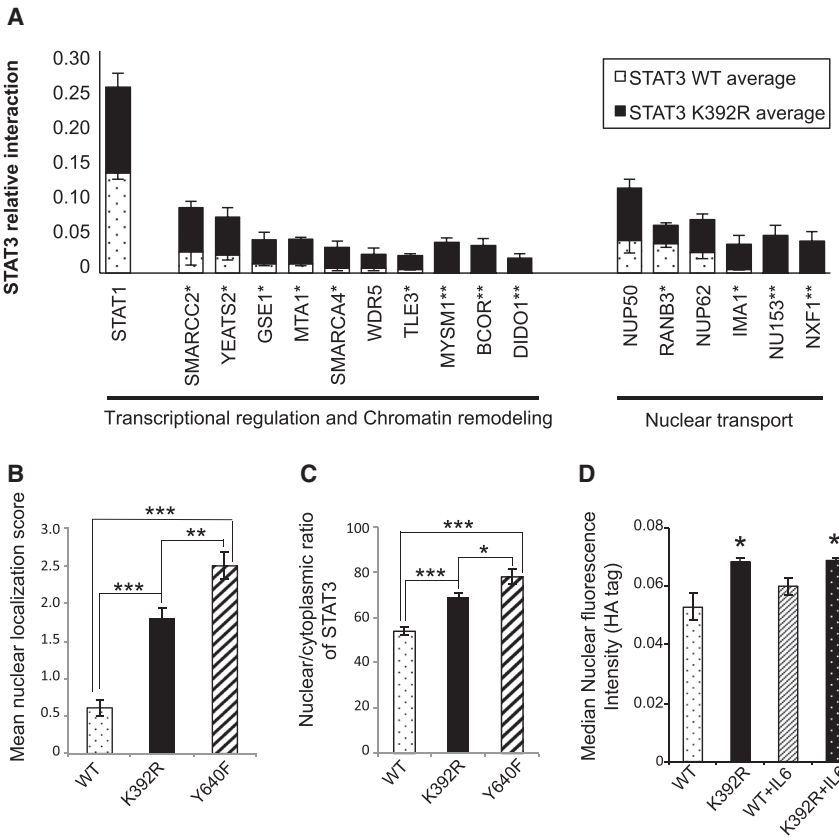


**Figure 6. K392R Mutation Increases STAT3 Nuclear Localization**

(A) Biotin proximity assay identifies interactions between STAT3 and proteins involved in transcriptional regulation (STAT1 [known STAT3 partner], GSE1, TLE3, MTA1, BCOR, and DIDO1), chromatin remodeling (SMARCC2, YEATS2, SMARCA4, WDR5, and MYSM1), and nuclear transport (NUP50, RANBP3, NUP62, IMA1, NU153, and NXF1). Compared to the STAT3 WT, $STAT^{K392R}$ in general shows significantly increased interactions with nuclear proteins and notably transport proteins involved in nuclear import, suggesting an increased nuclear translocation. *, significantly different interacting proteins; $p < 0.05$; Student's t test; n = 3. **, detected proteins interacting only with STAT3 K392R or WT.

(B) Nuclear localization of STAT3 determined by manual blinded scoring of HEK293 overexpressing STAT3 WT, STAT3 K392R, or STAT3 Y640F, a mutant with increased nuclear localization. n = 16–30 individually scored cells. Statistical analysis was performed with one-way ANOVA with Tukey's multiple comparison test. Differences between the conditions are marked in the figure. $^{**}p < 0.01$; $^{***}p < 0.001$.

(C) Nuclear localization of STAT3 determined by measuring nuclear to cytoplasmic ratio of STAT3 versions overexpressed in HEK293 cells as in (B). n = 26–30 individually measured cells. Statistical analysis was performed with one-way ANOVA with Tukey's multiple comparison test. Differences between the conditions are marked in the figure. $^{*}p < 0.05$; $^{***}p < 0.001$.

(D) Nuclear localization of STAT3 determined by quantification of nuclear intensity of stained STAT3 WT and STAT3 K392R-overexpressing HEK293 cells, treated or not with IL-6. Data represent mean ± SEM; n = 3 biological replicates. Analysis was performed on five random fields imaged per well, with an average of 63 nuclei/image, 315 nuclei/well, and 945 nuclei/condition. Statistical analysis was performed with one-way ANOVA with Tukey's multiple comparison test. Stars mark the differences between measured condition and WT STAT3. $^{*}p < 0.05$.

Thus, we hypothesize that $STAT3^{K392R}$ is shuttled more effectively into the nuclear compartment, and this was confirmed by immunocytochemical analysis of STAT3 localization (Figures 6B–6D).

### Transplanted *STAT3*$^{K392R}$ Cells Differentiate Preferentially into Alpha Cells

To study the functional outcome of the *STAT3*$^{K392R}$ mutation in mature endocrine cells, we transplanted control and *STAT3*$^{K392R}$-differentiated cells under the kidney capsule of immunodeficient non-obese diabetic (NOD)-severe combined immunodeficiency (SCID)-gamma (NSG) mice. Three months after transplantation, grafts presented organized cytoarchitecture (Figures 7A and 7B) with abundant endocrine cells. Closer examination of the endocrine cell numbers showed predominantly GCG+ cells at the expense of INS+ cells in the *STAT3*$^{K392R}$ grafts (Figure 7C). The percentage of double-positive GCG+/INS+ polyhormonal cells was overall low, 2.27% and 1.16% of total for *CTRL* and *STAT3*$^{K392R}$ grafts, respectively, and not significantly different. Interestingly, these results are concordant with the clinical features in the patient at birth, demonstrating normal levels of circulating glucagon but only traces of C-peptide (Otonkoski et al., 2000; unpublished data).

## DISCUSSION

This experimental project was stimulated by a unique experiment of nature: the identification of an activating STAT3 mutation in a patient with permanent neonatal diabetes, pancreatic hypoplasia, growth failure, and several organ-specific autoimmune features (Otonkoski et al., 2000; Flanagan et al., 2014; Haapaniemi et al., 2015). Previous reports have focused mainly on the immune system as the target of the pathology associated with activating STAT3 mutations. However, several clinical features, such as the pancreatic hypoplasia and primary growth failure, could also be due to organ-specific effects of the mutation outside the immune system. Using pancreatic differentiation of patient-derived iPSCs, we demonstrate that the K392R mutation in STAT3 leads to premature differentiation of pancreatic progenitors. This effect is mediated through activation of NEUROG3, a master regulator of endocrine pancreatic development. The mechanism does not involve activation of classical STAT3 signaling pathways but appears to be due to increased shuttling of the mutant STAT3 protein into the nucleus, where it can bind and induce the *NEUROG3* promoter.

NEUROG3 is a basic helix-loop-helix transcription factor acting as the master regulator of pancreatic endocrine cell

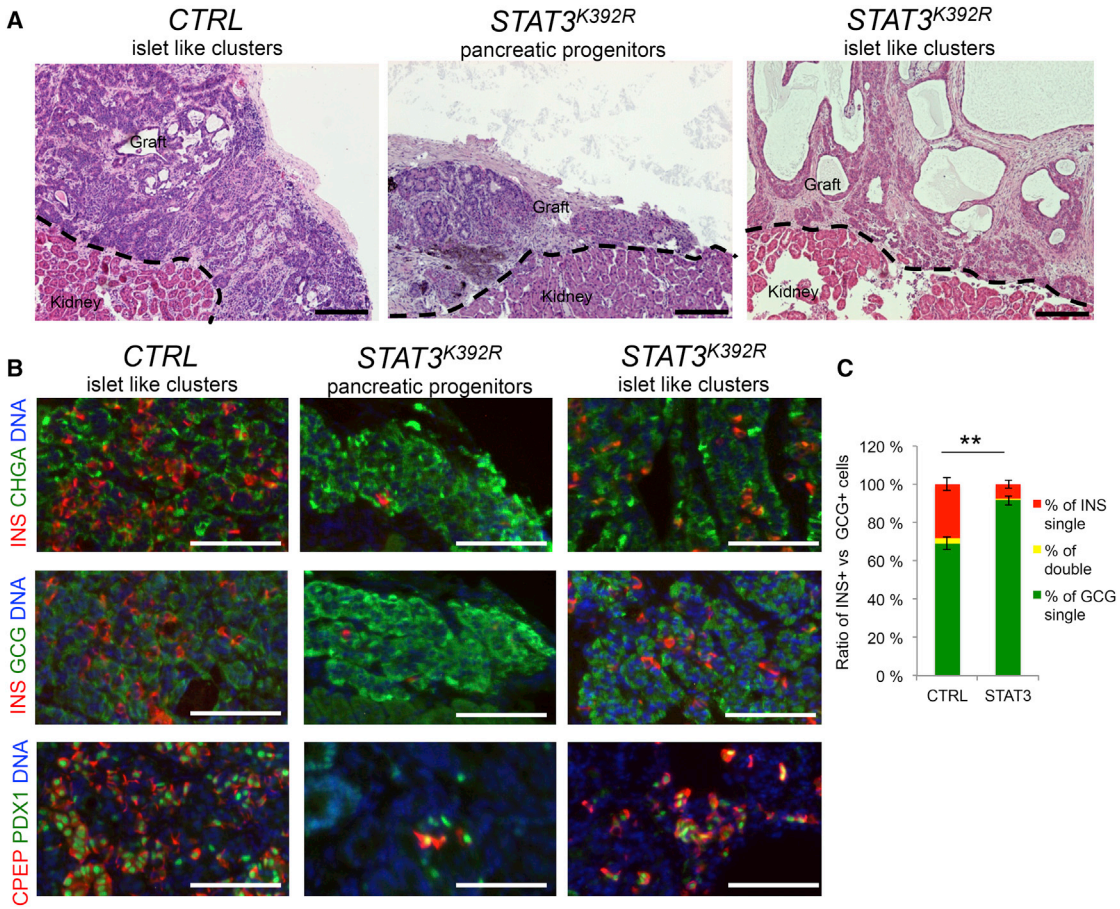


**Figure 7. Prematurely Differentiated *STAT*$^{K392R}$ Cells Form GCG-Positive Cells after Transplantation**

(A) Hematoxylene-Eosin (HE) staining of pancreatic grafts derived from *CTRL* (healthy donor) and *STAT3*$^{K392R}$ iPSCs grafts removed at 3 months after transplantation under the kidney capsule of NSG mice (borderline between kidney and graft tissue marked by a dashed line). Four grafts were produced using the 30-day, seven-stage protocol for islet-like aggregates (Figure 2; two derived from healthy-control iPSCs and two from mutant iPSCs) and four grafts using the 17-day, four-stage pancreatic progenitor protocol (Figure 1; two derived from healthy-control iPSCs and two from mutant iPSCs), totally eight different grafts, four per genotype. The scale bars represent 200 μm.

(B) Double immunohistochemistry of graft sections for INS + CHGA (top), INS+ GCG (middle), and PDX1 + C-PEPTIDE (CPEP) (bottom). The scale bars represent 100 μm.

(C) Quantification of relative proportion of INS+, GCG+, and double-positive cells in *CTRL* and *STAT3*$^{K392R}$ grafts (n = 4 individual grafts per genotype, totaling eight different grafts). Statistical analysis was performed with Student's t test; **p < 0.01.

differentiation. Lack of NEUROG3 leads to developmental failure of endocrine cells in mouse (Gradwohl et al., 2000; Schwitzgebel et al., 2000) and human (McGrath et al., 2015; Pinney et al., 2011; Rubio-Cabezas et al., 2011). The expression level of NEUROG3 is crucial for the endocrine commitment of the pancreatic progenitors (Wang et al., 2010), whereas its timing determines the allocation of the different endocrine cell types (Johansson et al., 2007). In support of this, forced overexpression of Neurog3 during early development results in pancreatic hypoplasia in transgenic mouse models (Apelqvist et al., 1999; Schwitzgebel et al., 2000) and biased differentiation of endocrine progenitors toward alpha cells (Johansson et al., 2007). Therefore, the abnormal NEUROG3 upregulation observed in patient-derived iPSCs would be expected to lead to pancreatic progenitor pool depletion, thereby explaining the pancreatic hypoplasia in the patient. More advanced differentiation of the patient cells in vitro and after transplantation revealed strongly biased differentiation toward alpha cells at the expense of beta cells (Figures 2 and 7). Similar biased differentiation has been previously reported in PSC-derived pancreatic progenitor grafts (Rezania et al., 2011, 2013). The expression of NEUROG3 before the onset of NKX6.1 in the pancreatic progenitors results in polyhormonal cells in vitro that differentiate into alpha cells after transplantation. This can be controlled if NEUROG3 is induced in progenitors expressing NKX6.1 (Nostro et al., 2015; Rezania et al., 2013; Russ et al., 2015). These observations on the premature induction of *NEUROG3* are consistent with our findings on the effect of *STAT3*$^{K392R}$ mutation.

Furthermore, these experimental results go well together with the clinical data, showing only traces of circulating C-peptide

(less than 0.05 nmol/L throughout life) but a normal level of plasma glucagon (77 ng/L at the age of 2 months and 124 ng/L at the age of 18 years), together with a rudimentary pancreas in MRI (Otonkoski et al., 2000). These findings are also entirely consistent with the transgenic mouse models of NEUROG3 overexpression in pancreatic progenitors (Apelqvist et al., 1999; Johansson et al., 2007).

NEUROG3 expression is activated by upstream transcription factors, such as PDX1, FOXA2, SOX9, HNF6, GLIS3, and HNF1B (Jacquemin et al., 2000; Kim et al., 2012; Lee et al., 2001; Oliver-Krasinski et al., 2009; Pan and Wright, 2011; Seymour et al., 2008; De Vas et al., 2015). In addition, Notch signaling regulates the levels of NEUROG3 post-transcriptionally through a lateral inhibition mechanism (Afelik and Jensen, 2013). The Notch downstream effector Hes1 regulates proliferation of pancreatic progenitors and endocrine differentiation (Pan and Wright, 2011), whereas inhibition of Notch results in premature differentiation of islet cells (Jensen et al., 2000). However, we did not detect any significant changes in the expression of NEUROG3 upstream regulators or in the genes associated with Notch signaling. A non-canonical Notch signaling axis involving phosphatidylinositol 3-kinase (PI3K)-Akt-mTOR, STAT3-Ser phosphorylation, and HES3 has also been suggested to control NEUROG3 activation (Masjkur et al., 2016), but we could not detect any changes in HES3 transcriptional levels in our experiments (data not shown). Thus, the premature upregulation of NEUROG3 caused by the STAT3 mutation does not seem to be mediated by perturbations in the known developmental mechanisms controlling NEUROG3.

STAT3 signaling has been studied in the context of pancreatic plasticity in diabetic mouse models, where it mediates the activation of Neurog3 in acinar cells that reprogram to beta cells (Baeyens et al., 2006, 2014). In mice rendered diabetic by selective beta cell destruction with alloxan, treatment with epidermal growth factor (EGF) and ciliary neurotrophic factor (CNTF) (a STAT3 signaling pathway ligand) resulted in increased phosphorylation of STAT3, leading to the upregulation of Neurog3 (Baeyens et al., 2014). Similar results have been shown in human exocrine pancreatic cells transduced with constitutively active forms of STAT3 and MAPK (Lemper et al., 2015) and in the human ductal cell line PANC1 treated with proinflammatory cytokines (Valdez et al., 2016). Using a global bioinformatic approach and a causal reasoning algorithm, Gutteridge and colleagues suggested that STAT3 signaling pathway is involved in the activation of NEUROG3 in differentiating human embryonic stem cells (Gutteridge et al., 2013). The studies described above show that JAK-mediated phosphorylation of STAT3 results in *NEUROG3* transcriptional activation. However, several lines of evidence suggest that mutant STAT3$^{K392R}$ exerts its effects independently of phosphorylation status. Thus, stimulation of the pancreatic endoderm cells with IL-6 or LIF resulted in Y705 STAT3 phosphorylation but did not increase NEUROG3 activation in our experiments (Figures 4C, 4D, and S7). This is consistent with the retention of increased transcriptional activity in the Y705F mutant STAT3$^{K392R}$ (Figure S7B). Interestingly, the nuclear import of STAT3 is independent of tyrosine phosphorylation (Liu et al., 2005), and STAT3 has been suggested to function as a transcriptional activator and a chromatin organizer in its unphosphorylated form (Sehgal, 2008; Timofeeva et al., 2012).

STAT3 has been reported to bind to the *Neurog3* promoter in differentiating mouse spermatogonial cells (Kaucher et al., 2012). We demonstrate by oligonucleotide pull-down and luciferase reporter assay that both WT and STAT3$^{K392R}$ bind to the *NEUROG3* promoter independently of STAT3 phosphorylation status, further suggesting the role of unphosphorylated STAT3 in regulating *NEUROG3* (Timofeeva et al., 2012).

Biotin proximity assay showed increased interaction of mutant STAT3 with several nuclear pore complex proteins, transcriptional regulators, and chromatin remodelers. These differential interactions suggest an increased nuclear translocation of the mutant protein, which was further confirmed by quantitative immunofluorescence microscopy (Figure 6B). Although the location of the mutation within the DNA-binding domain (DBD) of STAT3 would suggest an effect on STAT3 DNA-binding properties, our data show that both WT and STAT3$^{K392R}$ bind to DNA with similar affinities. Collectively, our results suggest strongly that increased nuclear localization of STAT3$^{K392R}$ is the main mechanism for increased activation of NEUROG3.

In summary, our study highlights a pathogenetic mechanism associated with organ-specific dysregulation of a centrally important signal transducer, STAT3. The pathogenetic mechanisms of activating STAT3 mutations have previously been studied in the context of the immune and hematopoietic systems (Koskela et al., 2012). However, our results demonstrate that, in addition to the early onset autoimmunity, the same mutation leads to a primary developmental defect in pancreatic organogenesis. Further studies will be needed to establish whether a similar developmental mechanism in the bone growth plates may underline the severe primary overall growth defect of the patient. Finally, our experimental approach demonstrates the versatility of iPSCs combined with genome editing as powerful tools that can be applied to elucidate organ-specific pathogenetic mechanisms. Whereas this study relies on the derivation of iPSCs from a single patient carrying the STAT3$^{K392R}$ mutation, follow-up studies are needed with other activating STAT3 mutations, using both patient-derived iPSCs and engineering of the mutations in standard human pluripotent stem cell (hPSC) lines.

## EXPERIMENTAL PROCEDURES

Additional details are provided in Supplemental Experimental Procedures.

### Patient Samples and the Use of Animals

Human induced pluripotent stem cell (hiPSC) lines used in this study were generated after informed consent approved by the Coordinating Ethics Committee of the Helsinki and Uusimaa Hospital District (no. 423/13/03/00/08). Animal care and experiments were approved by the National Animal Experiment Board in Finland (ESAVI/9978/04.10.07/2014). NSG (Jackson Laboratories; 005557) male mice, aged 3–12 months, were used for this study.

### Cell Culture

iPSC lines HEL72.1, HEL72A, and HEL72D were derived from STAT3$^{K392R}$ patient skin fibroblasts using retroviral-based reprogramming as described elsewhere (Toivonen et al., 2013a). Human iPSC line HEL47.2 (derived from 83-year-old male skin fibroblast), HEL24.3, and HEL46.11 (derived from human neonatal foreskin fibroblast) were reprogrammed using Sendai virus technology as described elsewhere (Trokovic et al., 2015a, 2015b).

HEL47.2, HEL24.3, and HEL46.11, together with human embryonic stem cell (ESC) line H9 (Thomson et al., 1998), were used as healthy-donor controls.

Undifferentiated cells were cultured on Matrigel (BD Biosciences)-coated plates in E8 medium (Life Technologies; A1517001) and passaged with 5 mM EDTA (Life Technologies; 15575-038).

### Differentiation

The cells were differentiated using a 17-day protocol (see Figure 1A) described earlier (Toivonen et al., 2013b) or 30-day protocol (see Figure 2A). Additional details are provided in Supplemental Experimental Procedures.

### Genome Editing

Two million patient-derived iPSCs were electroporated with 6 μg of CAG-Cas9-T2A-EGFP-ires-Puro (deposited in Addgene, plasmid no. 78311, together with detailed protocols for its use), 500 ng of gRNA-PCR STAT3.3 product, and 6 μg of dsDNA correction template PCR product using Neon Transfection system (Thermo Fisher; 1,100 V; 20 ms; two pulses). Cells were single-cell sorted, expanded, and screened for recombination with the donor template. Positive clones were validated by Sanger sequencing. See also Supplemental Experimental Procedures.

### Biotin Proximity Assay, Mass Spectrometry, Protein Identification, and Quantification

For each BioID analysis, approximately 5 × 10E7 HEK293 cells were induced with 2 μg/mL tetracycline (for STAT3 WT and STAT3K392R expression induction) and 50 μM biotin (for activation of the BirA -biotin ligase) for 24 hr. Cells were harvested and lysates prepared and loaded to Strep-Tactin Sepharose beads (400 μL 50% Slurry; IBA). Bound proteins were eluted with 2 × 300 μL freshly prepared 0.5 mM D-biotin (Thermo Fisher Scientific).

Liquid chromatography-mass spectrometry (LC-MS/MS) and data analysis was performed as described earlier (Kämpjärvi et al., 2016). SEQUEST search algorithm in Proteome Discoverer software (Thermo Fisher Scientific) was used for peak extraction and protein identification. Proteins detected with <20% frequency or 3-fold higher abundance (spectral counts) compared to the controls were classified as high-confidence interacting proteins. Proteins were identified and quantified using Andromeda search engine combined with MaxQuant proteomics software (Cox et al., 2011; Cox and Mann, 2008). Raw data were searched against the human component of the UniProtKB database (release 2014_11) complemented with trypsin and tag sequences.

### Statistical Analysis

Statistical analysis was performed with Student's unpaired t test or one-way ANOVA followed by Tukey's multiple comparison post hoc test using GraphPad Prism software (GraphPad Software). Separation between homoscedastic (equal variance) and heteroscedastic (unequal variance) type of t test was analyzed with F test. p values under 0.05 were considered statistically significant (*$p < 0.05$; **$p < 0.01$; ***$p < 0.001$).

## ACCESSION NUMBERS

The accession number for the RNA sequencing results data reported in this paper is SRA: PRJNA379179, study SRP101885, submission SUB2461615 (https://www.ncbi.nlm.nih.gov/bioproject/PRJNA379179).

## SUPPLEMENTAL INFORMATION

Supplemental Information includes Supplemental Experimental Procedures, seven figures, and two tables and can be found with this article online at http://dx.doi.org/10.1016/j.celrep.2017.03.055.

## AUTHOR CONTRIBUTIONS

Conceptualization, J.S.-V., D.B., and T.O.; Methodology, J.S.-V., D.B., S.E., H.G., and J.U.; Investigation, J.S.-V., D.B., S.E., H.G., J.U., M.A.R., A.M., J.S., M.K., S.K., C.V., and C.A.; Resources, R.D.H., M.V., O.S., N.G.M., and T.O.; Writing – Original Draft, J.S.-V., D.B., and T.O.; Writing – Review & Editing, J.S.-V., D.B., N.G.M., and T.O.; Supervision, O.S., R.D.H., M.V., N.G.M., and T.O.; Funding Acquisition, K.W. and T.O.

## ACKNOWLEDGMENTS

Anni Laitinen, Eila Korhonen, Hazem Ibrahim, Väinö Lithovius, Noora Aarnio, Jessica Chaffey, and Niina Siiskonen are thanked for their professional technical assistance. We thank Elena Senís (Vall d'Hebron Institute of Oncology) for advice on T7 endonuclease assay. We are grateful to Ras Trokovic and Milla Mikkola for providing iPSC (HEL72.1, HEL72A, and HEL72D) lines. D.B. is a member of the Doctoral School of Health Sciences at University of Helsinki. This project was funded by the Academy of Finland (grant number 257157) Sigrid Jusélius Foundation, Novo Nordisk Foundation (grant numbers NNF16OC0021090, NNF15OC0016426, NNF14OC0010719, and NNF13OC0005565), the EU 7FP Integrated project BETACURE, the Diabetes Research Foundation, and Diabetes UK.

Received: May 13, 2016
Revised: February 10, 2017
Accepted: March 17, 2017
Published: April 11, 2017

## REFERENCES

Achuta, V.S., Grym, H., Putkonen, N., Louhivuori, V., Kärkkäinen, V., Koistinaho, J., Roybon, L., and Castrén, M.L. (2017). Metabotropic glutamate receptor 5 responses dictate differentiation of neural progenitors to NMDA-responsive cells in fragile X syndrome. Dev. Neurobiol. *77*, 438–453.

Afelik, S., and Jensen, J. (2013). Notch signaling in the pancreas: patterning and cell fate specification. Wiley Interdiscip. Rev. Dev. Biol. *2*, 531–544.

Apelqvist, Å., Li, H., Sommer, L., Beatus, P., Anderson, D.J., Honjo, T., Hrabě de Angelis, M., Lendahl, U., and Edlund, H. (1999). Notch signalling controls pancreatic cell differentiation. Nature *400*, 877–881.

Baeyens, L., Bonné, S., German, M.S., Ravassard, P., Heimberg, H., and Bouwens, L. (2006). Ngn3 expression during postnatal in vitro beta cell neogenesis induced by the JAK/STAT pathway. Cell Death Differ. *13*, 1892–1899.

Baeyens, L., Lemper, M., Leuckx, G., De Groef, S., Bonfanti, P., Stangé, G., Shemer, R., Nord, C., Scheel, D.W., Pan, F.C., et al. (2014). Transient cytokine treatment induces acinar cell reprogramming and regenerates functional beta cell mass in diabetic mice. Nat. Biotechnol. *32*, 76–83.

Choi, J., Lee, S., Mallard, W., Clement, K., Tagliazucchi, G.M., Lim, H., Choi, I.Y., Ferrari, F., Tsankov, A.M., Pop, R., et al. (2015). A comparison of genetically matched cell lines reveals the equivalence of human iPSCs and ESCs. Nat. Biotechnol. *33*, 1173–1181.

Cox, J., and Mann, M. (2008). MaxQuant enables high peptide identification rates, individualized p.p.b.-range mass accuracies and proteome-wide protein quantification. Nat. Biotechnol. *26*, 1367–1372.

Cox, J., Neuhauser, N., Michalski, A., Scheltema, R.A., Olsen, J.V., and Mann, M. (2011). Andromeda: a peptide search engine integrated into the MaxQuant environment. J. Proteome Res. *10*, 1794–1805.

De Franco, E., and Ellard, S. (2015). Genome, exome, and targeted next-generation sequencing in neonatal diabetes. Pediatr. Clin. North Am. *62*, 1037–1053.

De Vas, M.G., Kopp, J.L., Heliot, C., Sander, M., Cereghini, S., and Haumaitre, C. (2015). Hnf1b controls pancreas morphogenesis and the generation of Ngn3+ endocrine progenitors. Development *142*, 871–882.

Flanagan, S.E., Haapaniemi, E., Russell, M.A., Caswell, R., Lango Allen, H., De Franco, E., McDonald, T.J., Rajala, H., Ramelius, A., Barton, J., et al. (2014). Activating germline mutations in STAT3 cause early-onset multi-organ autoimmune disease. Nat. Genet. *46*, 812–814.

Gorogawa, S., Fujitani, Y., Kaneto, H., Hazama, Y., Watada, H., Miyamoto, Y., Takeda, K., Akira, S., Magnuson, M.A., Yamasaki, Y., et al. (2004). Insulin secretory defects and impaired islet architecture in pancreatic beta-cell-

specific STAT3 knockout mice. Biochem. Biophys. Res. Commun. *319*, 1159–1170.

Gradwohl, G., Dierich, A., LeMeur, M., and Guillemot, F. (2000). neurogenin3 is required for the development of the four endocrine cell lineages of the pancreas. Proc. Natl. Acad. Sci. USA *97*, 1607–1611.

Gutteridge, A., Rukstalis, J.M., Ziemek, D., Tié, M., Ji, L., Ramos-Zayas, R., Nardone, N.A., Norquay, L.D., Brenner, M.B., Tang, K., et al. (2013). Novel pancreatic endocrine maturation pathways identified by genomic profiling and causal reasoning. PLoS ONE *8*, e56024.

Haapaniemi, E.M., Kaustio, M., Rajala, H.L.M., van Adrichem, A.J., Kainulainen, L., Glumoff, V., Doffinger, R., Kuusanmäki, H., Heiskanen-Kosma, T., Trotta, L., et al. (2015). Autoimmunity, hypogammaglobulinemia, lymphoproliferation, and mycobacterial disease in patients with activating mutations in STAT3. Blood *125*, 639–648.

Jacquemin, P., Durviaux, S.M., Jensen, J., Godfraind, C., Gradwohl, G., Guillemot, F., Madsen, O.D., Carmeliet, P., Dewerchin, M., Collen, D., et al. (2000). Transcription factor hepatocyte nuclear factor 6 regulates pancreatic endocrine cell differentiation and controls expression of the proendocrine gene ngn3. Mol. Cell. Biol. *20*, 4445–4454.

Jennings, R.E., Berry, A.A., Strutt, J.P., Gerrard, D.T., and Hanley, N.A. (2015). Human pancreas development. Development *142*, 3126–3137.

Jensen, J., Heller, R.S., Funder-Nielsen, T., Pedersen, E.E., Lindsell, C., Weinmaster, G., Madsen, O.D., and Serup, P. (2000). Independent development of pancreatic alpha- and beta-cells from neurogenin3-expressing precursors: a role for the notch pathway in repression of premature differentiation. Diabetes *49*, 163–176.

Johansson, K.A., Dursun, U., Jordan, N., Gu, G., Beermann, F., Gradwohl, G., and Grapin-Botton, A. (2007). Temporal control of neurogenin3 activity in pancreas progenitors reveals competence windows for the generation of different endocrine cell types. Dev. Cell *12*, 457–465.

Kämpjärvi, K., Kim, N.H., Keskitalo, S., Clark, A.D., von Nandelstadh, P., Turunen, M., Heikkinen, T., Park, M.J., Mäkinen, N., Kivinummi, K., et al. (2016). Somatic MED12 mutations in prostate cancer and uterine leiomyomas promote tumorigenesis through distinct mechanisms. Prostate *76*, 22–31.

Kaucher, A.V., Oatley, M.J., and Oatley, J.M. (2012). NEUROG3 is a critical downstream effector for STAT3-regulated differentiation of mammalian stem and progenitor spermatogonia. Biol. Reprod. *86*, 164, 1–11.

Kim, Y.-S., Kang, H.S., Takeda, Y., Hom, L., Song, H.-Y., Jensen, J., and Jetten, A.M. (2012). Glis3 regulates neurogenin 3 expression in pancreatic β-cells and interacts with its activator, Hnf6. Mol. Cells *34*, 193–200.

Koskela, H.L.M., Eldfors, S., Ellonen, P., van Adrichem, A.J., Kuusanmäki, H., Andersson, E.I., Lagström, S., Clemente, M.J., Olson, T., Jalkanen, S.E., et al. (2012). Somatic STAT3 mutations in large granular lymphocytic leukemia. N. Engl. J. Med. *366*, 1905–1913.

Kostromina, E., Gustavsson, N., Wang, X., Lim, C.-Y., Radda, G.K., Li, C., and Han, W. (2010). Glucose intolerance and impaired insulin secretion in pancreas-specific signal transducer and activator of transcription-3 knockout mice are associated with microvascular alterations in the pancreas. Endocrinology *151*, 2050–2059.

Kostromina, E., Wang, X., and Han, W. (2013). Altered islet morphology but normal islet secretory function in vitro in a mouse model with microvascular alterations in the pancreas. PLoS ONE *8*, e71277.

Kyttälä, A., Moraghebi, R., Valensisi, C., Kettunen, J., Andrus, C., Pasumarthy, K.K., Nakanishi, M., Nishimura, K., Ohtaka, M., Weltner, J., et al. (2016). Genetic variability overrides the impact of parental cell type and determines iPSC differentiation potential. Stem Cell Reports *6*, 200–212.

Lee, J.-Y., and Hennighausen, L. (2005). The transcription factor Stat3 is dispensable for pancreatic beta-cell development and function. Biochem. Biophys. Res. Commun. *334*, 764–768.

Lee, J.C., Smith, S.B., Watada, H., Lin, J., Scheel, D., Wang, J., Mirmira, R.G., and German, M.S. (2001). Regulation of the pancreatic pro-endocrine gene neurogenin3. Diabetes *50*, 928–936.

Lemper, M., Leuckx, G., Heremans, Y., German, M.S., Heimberg, H., Bouwens, L., and Baeyens, L. (2015). Reprogramming of human pancreatic exocrine cells to β-like cells. Cell Death Differ. *22*, 1117–1130.

Liu, L., McBride, K.M., and Reich, N.C. (2005). STAT3 nuclear import is independent of tyrosine phosphorylation and mediated by importin-alpha3. Proc. Natl. Acad. Sci. USA *102*, 8150–8155.

Masjkur, J., Poser, S.W., Nikolakopoulou, P., Chrousos, G., McKay, R.D., Bornstein, S.R., Jones, P.M., and Androutsellis-Theotokis, A. (2016). Endocrine pancreas development and regeneration: noncanonical ideas from neural stem cell biology. Diabetes *65*, 314–330.

McGrath, P.S., Watson, C.L., Ingram, C., Helmrath, M.A., and Wells, J.M. (2015). The basic helix-loop-helix transcription factor NEUROG3 is required for development of the human endocrine pancreas. Diabetes *64*, 2497–2505.

Mfopou, J.K., Chen, B., Mateizel, I., Sermon, K., and Bouwens, L. (2010). Noggin, retinoids, and fibroblast growth factor regulate hepatic or pancreatic fate of human embryonic stem cells. Gastroenterology *138*, 2233–2245.

Murphy, R., Ellard, S., and Hattersley, A.T. (2008). Clinical implications of a molecular genetic classification of monogenic beta-cell diabetes. Nat. Clin. Pract. Endocrinol. Metab. *4*, 200–213.

Nostro, M.C., Sarangi, F., Ogawa, S., Holtzinger, A., Corneo, B., Li, X., Micallef, S.J., Park, I.-H., Basford, C., Wheeler, M.B., et al. (2011). Stage-specific signaling through TGFβ family members and WNT regulates patterning and pancreatic specification of human pluripotent stem cells. Development *138*, 861–871.

Nostro, M.C., Sarangi, F., Yang, C., Holland, A., Elefanty, A.G., Stanley, E.G., Greiner, D.L., and Keller, G. (2015). Efficient generation of NKX6-1+ pancreatic progenitors from multiple human pluripotent stem cell lines. Stem Cell Reports *4*, 591–604.

O'Shea, J.J., and Plenge, R. (2012). JAK and STAT signaling molecules in immunoregulation and immune-mediated disease. Immunity *36*, 542–550.

O'Shea, J.J., Holland, S.M., and Staudt, L.M. (2013). JAKs and STATs in immunity, immunodeficiency, and cancer. N. Engl. J. Med. *368*, 161–170.

Oliver-Krasinski, J.M., Kasner, M.T., Yang, J., Crutchlow, M.F., Rustgi, A.K., Kaestner, K.H., and Stoffers, D.A. (2009). The diabetes gene Pdx1 regulates the transcriptional network of pancreatic endocrine progenitor cells in mice. J. Clin. Invest. *119*, 1888–1898.

Otonkoski, T., Roivainen, M., Vaarala, O., Dinesen, B., Leipälä, J.A., Hovi, T., and Knip, M. (2000). Neonatal type I diabetes associated with maternal echovirus 6 infection: a case report. Diabetologia *43*, 1235–1238.

Pagliuca, F.W., Millman, J.R., Gürtler, M., Segel, M., Van Dervort, A., Ryu, J.H., Peterson, Q.P., Greiner, D., and Melton, D.A. (2014). Generation of functional human pancreatic β cells in vitro. Cell *159*, 428–439.

Pan, F.C., and Wright, C. (2011). Pancreas organogenesis: from bud to plexus to gland. Dev. Dyn. *240*, 530–565.

Pilati, C., Amessou, M., Bihl, M.P., Balabaud, C., Nhieu, J.T., Paradis, V., Nault, J.C., Izard, T., Bioulac-Sage, P., Couchy, G., et al. (2011). Somatic mutations activating STAT3 in human inflammatory hepatocellular adenomas. J. Exp. Med. *208*, 1359–1366.

Pinney, S.E., Oliver-Krasinski, J., Ernst, L., Hughes, N., Patel, P., Stoffers, D.A., Russo, P., and De León, D.D. (2011). Neonatal diabetes and congenital malabsorptive diarrhea attributable to a novel mutation in the human neurogenin-3 gene coding sequence. J. Clin. Endocrinol. Metab. *96*, 1960–1965.

Puri, S., Folias, A.E., and Hebrok, M. (2015). Plasticity and dedifferentiation within the pancreas: development, homeostasis, and disease. Cell Stem Cell *16*, 18–31.

Rezania, A., Riedel, M.J., Wideman, R.D., Karanu, F., Ao, Z., Warnock, G.L., and Kieffer, T.J. (2011). Production of functional glucagon-secreting α-cells from human embryonic stem cells. Diabetes *60*, 239–247.

Rezania, A., Bruin, J.E., Xu, J., Narayan, K., Fox, J.K., O'Neil, J.J., and Kieffer, T.J. (2013). Enrichment of human embryonic stem cell-derived NKX6.1-expressing pancreatic progenitor cells accelerates the maturation of insulin-secreting cells in vivo. Stem Cells *31*, 2432–2442.

Rezania, A., Bruin, J.E., Arora, P., Rubin, A., Batushansky, I., Asadi, A., O'Dwyer, S., Quiskamp, N., Mojibian, M., Albrecht, T., et al. (2014). Reversal of diabetes with insulin-producing cells derived in vitro from human pluripotent stem cells. Nat. Biotechnol. *32*, 1121–1133.

Roux, K.J., Kim, D.I., Raida, M., and Burke, B. (2012). A promiscuous biotin ligase fusion protein identifies proximal and interacting proteins in mammalian cells. J. Cell Biol. *196*, 801–810.

Rubio-Cabezas, O., Jensen, J.N., Hodgson, M.I., Codner, E., Ellard, S., Serup, P., and Hattersley, A.T. (2011). Permanent neonatal diabetes and enteric anendocrinosis associated with biallelic mutations in NEUROG3. Diabetes *60*, 1349–1353.

Russ, H.A., Parent, A.V., Ringler, J.J., Hennings, T.G., Nair, G.G., Shveygert, M., Guo, T., Puri, S., Haataja, L., Cirulli, V., et al. (2015). Controlled induction of human pancreatic progenitors produces functional beta-like cells in vitro. EMBO J. *34*, 1759–1772.

Schwitzgebel, V.M., Scheel, D.W., Conners, J.R., Kalamaras, J., Lee, J.E., Anderson, D.J., Sussel, L., Johnson, J.D., and German, M.S. (2000). Expression of neurogenin3 reveals an islet cell precursor population in the pancreas. Development *127*, 3533–3542.

Sehgal, P.B. (2008). Paradigm shifts in the cell biology of STAT signaling. Semin. Cell Dev. Biol. *19*, 329–340.

Seymour, P.A., Freude, K.K., Dubois, C.L., Shih, H.-P., Patel, N.A., and Sander, M. (2008). A dosage-dependent requirement for Sox9 in pancreatic endocrine cell formation. Dev. Biol. *323*, 19–30.

Takeda, K., Noguchi, K., Shi, W., Tanaka, T., Matsumoto, M., Yoshida, N., Kishimoto, T., and Akira, S. (1997). Targeted disruption of the mouse Stat3 gene leads to early embryonic lethality. Proc. Natl. Acad. Sci. USA *94*, 3801–3804.

Thomson, J.A., Itskovitz-Eldor, J., Shapiro, S.S., Waknitz, M.A., Swiergiel, J.J., Marshall, V.S., and Jones, J.M. (1998). Embryonic stem cell lines derived from human blastocysts. Science *282*, 1145–1147.

Timofeeva, O.A., Chasovskikh, S., Lonskaya, I., Tarasova, N.I., Khavrutskii, L., Tarasov, S.G., Zhang, X., Korostyshevskiy, V.R., Cheema, A., Zhang, L., et al. (2012). Mechanisms of unphosphorylated STAT3 transcription factor binding to DNA. J. Biol. Chem. *287*, 14192–14200.

Toivonen, S., Ojala, M., Hyysalo, A., Ilmarinen, T., Rajala, K., Pekkanen-Mattila, M., Äänismaa, R., Lundin, K., Palgi, J., Weltner, J., et al. (2013a). Comparative analysis of targeted differentiation of human induced pluripotent stem cells (hiPSCs) and human embryonic stem cells reveals variability associated with incomplete transgene silencing in retrovirally derived hiPSC lines. Stem Cells Transl. Med. *2*, 83–93.

Toivonen, S., Lundin, K., Balboa, D., Ustinov, J., Tamminen, K., Palgi, J., Trokovic, R., Tuuri, T., and Otonkoski, T. (2013b). Activin A and Wnt-dependent specification of human definitive endoderm cells. Exp. Cell Res. *319*, 2535–2544.

Trokovic, R., Weltner, J., and Otonkoski, T. (2015a). Generation of iPSC line HEL47.2 from healthy human adult fibroblasts. Stem Cell Res. (Amst.) *15*, 263–265.

Trokovic, R., Weltner, J., and Otonkoski, T. (2015b). Generation of iPSC line HEL24.3 from human neonatal foreskin fibroblasts. Stem Cell Res. (Amst.) *15*, 266–268.

Valdez, I.A., Dirice, E., Gupta, M.K., Shirakawa, J., Teo, A.K.K., and Kulkarni, R.N. (2016). Proinflammatory cytokines induce endocrine differentiation in pancreatic ductal cells via STAT3-dependent NGN3 activation. Cell Rep. *15*, 460–470.

Wang, S., Yan, J., Anderson, D.A., Xu, Y., Kanal, M.C., Cao, Z., Wright, C.V., and Gu, G. (2010). Neurog3 gene dosage regulates allocation of endocrine and exocrine cell fates in the developing mouse pancreas. Dev. Biol. *339*, 26–37.

WHO (2016). Global report on diabetes. http://www.who.int/diabetes/global-report/en.